

Valley splitting of AlAs two-dimensional electrons in a perpendicular magnetic field

Y. P. Shkolnikov, E. P. De Poortere, E. Tutuc, and M. Shayegan

Department of Electrical Engineering, Princeton University, Princeton, New Jersey 08544

(Dated: November 18, 2018)

By measuring the angles at which the Landau levels overlap in tilted magnetic fields (the coincidence method), we determine the splitting of the conduction-band valleys in high-mobility two-dimensional (2D) electrons confined to AlAs quantum wells. The data reveal that, while the valleys are nearly degenerate in the absence of magnetic field, they split as a function of perpendicular magnetic field. The splitting appears to depend primarily on the magnitude of the perpendicular component of the magnetic field, suggesting electron-electron interaction as its origin.

PACS numbers: 73.21, 73.23, 73.43

In many semiconductors, the energy dispersion of the conduction band contains more than one minimum, or valley. Examples include Si and AlAs, where electrons occupy pockets near or at the equivalent X-points of the Brillouin zone. One of the long-standing and controversial problems in the physics of two-dimensional electron systems (2DESs) in such semiconductors has been the nature of valley splitting, i.e., the lifting of this valley degeneracy. While it is clear that mechanisms that break the symmetry of the crystal potential, such as uniaxial strain, can lift the degeneracy, it has remained controversial whether interaction between the electrons can also lead to a splitting [1]. In this Letter, we report measurements of transport in low disorder 2DESs in modulation-doped AlAs quantum wells, which provide clear evidence for the dependence of valley splitting on the applied perpendicular magnetic field (B_{\perp}). The data reveal that at zero magnetic field the electrons occupy two nearly-degenerate in-plane conduction-band valleys. With the application of B_{\perp} , we observe a splitting of the valley energies that increases monotonically with B_{\perp} and is essentially independent of the parallel component of the magnetic field (B_{\parallel}). This suggests that electron-electron interaction is responsible for the splitting.

We performed experiments on 2DESs confined to modulation doped AlAs quantum wells grown by molecular beam epitaxy on (100) GaAs substrates. In these samples, the AlAs quantum well is flanked by undoped and Si-doped layers of $\text{Al}_{0.4}\text{Ga}_{0.6}\text{As}$ [2]. We studied three samples with two different quantum well widths: 150Å for S1 and S3, and 110Å for S2. In bulk AlAs, electrons occupy three valleys that are located at X-point (rather than at Δ -point as in Si) of the Brillouin zone. Previous studies [3, 4, 5, 6] have indicated that strain due to lattice mismatch between AlAs quantum well and GaAs substrate leads to a lifting in energy and depopulation of the out-of-plane valley in AlAs quantum wells wider than 60Å. Consistent with these studies, the 2DES in our samples occupies two valleys whose principal axes lie in the 2D plane. In these remaining valleys, the cyclotron electron effective mass m^* is 0.46 (in units of the free electron mass, m_0) and the band g-factor g_b is 2. We measured

the magnetoresistance of the samples in L-shaped Hall bars aligned with [001] and [010] directions. Using illumination and front/back gate biasing, we were able to vary the 2D electron density n between 4.0×10^{11} and $9.6 \times 10^{11} \text{ cm}^{-2}$. At 30mK, the electron mobility of our samples was as high as 250,000 cm^2/Vs .

To measure the valley splitting (ΔE_V) as a function of magnetic field, we utilize the coincidence method [7]. This technique makes use of the difference in the magnetic field dependencies of the orbital and spin energies, and has been widely used to measure the spin-splitting and the effective g-factor in 2D systems. In a 2D system in a strong magnetic field, quantization of the orbital motion leads to the formation of Landau levels (LLs). The energy separation between the LLs is equal to the cyclotron energy, which, in an ideal 2D system equals $\hbar e B_{\perp} / (m^* m_0)$ and therefore depends only on B_{\perp} . Thanks to the Zeeman coupling, each LL splits into two energy levels, one for each polarization of spin. The energy separation between these levels, the Zeeman energy, is generally a function of the total magnetic field (B_{tot}) and is equal to $|g^*| \mu_B B_{tot}$ where μ_B is Bohr magneton and g^* is the effective g-factor. In a typical coincidence measurement, the 2D sample is placed in a magnetic field whose direction makes an angle θ with the normal to the 2D plane. The Zeeman energy is then measured (in units of the cyclotron energy) from the values of θ at which every other magnetoresistance minima disappear; the disappearance is the result of the overlap, at the Fermi energy, between two energy levels associated with opposite spin. Now, in a two-valley system, yet another splitting appears: each spin-resolved level splits in two levels, separated in energy by ΔE_V , corresponding to each of the valleys. In our measurements presented here, by carefully monitoring θ at which magnetoresistance minima disappear, we are able to determine both the Zeeman- and valley-splittings.

We first present data to establish that, at low magnetic fields, the 2D electrons in our samples occupy two nearly-degenerate valleys. Magnetoresistivity ρ_{xx} as a function of B_{\perp} (at zero B_{\parallel}) for sample S1 at a density of $n = 9.2 \times 10^{11} \text{ cm}^{-2}$ is shown in Fig. 1 [9]. Strong minima in ρ_{xx}

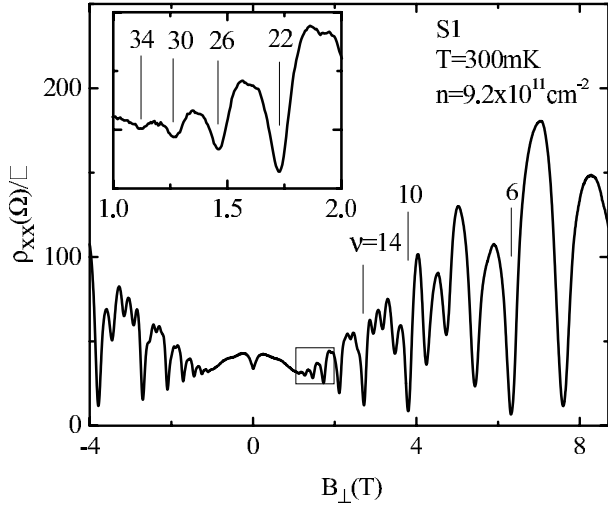


FIG. 1: Magnetoresistivity ρ_{xx} as a function of perpendicular magnetic field B_{\perp} for AlAs 2D electrons in sample S1. At low B_{\perp} , ρ_{xx} in the inset shows strong minima at every fourth filling factor ν , indicating a fourfold degeneracy of the Landau levels (2 for spin and 2 for valley). At higher B_{\perp} , all minima become stronger than their $(\nu+4)$ counterpart, implying that both spin- and valley-splitting increase with B_{\perp} .

occur at every fourth Landau level filling factor ν , which indicates a fourfold degeneracy of the Landau levels (two for spin and two for valley) [10]. This degeneracy can be clearly seen in the Fourier transform of ρ_{xx} vs. $1/B_{\perp}$ data, shown in the inset to Fig. 2 for sample S2 at a density of $7.9 \times 10^{11} \text{ cm}^{-2}$. The frequency of a peak in the Fourier transform can be converted to a 2D density by multiplying by e/h , where e is the electron charge and h is the Planck constant. The presence of a peak (square symbol) at the frequency equal to one quarter of the frequency associated with the total density confirms the spin- and valley-degeneracy at low B_{\perp} . We assign the other peaks in the Fourier transform to the spin- and/or valley-resolved oscillations which are observed at higher B_{\perp} [11].

In Fig. 2 we show a plot of the measured peak positions in Fourier transforms as we change the density in S2 via a front-gate bias. The valley/spin degeneracies persist at all n and, as the density is decreased, all the peak positions linearly decrease and extrapolate to approximately zero in the $n = 0$ limit. It is particularly noteworthy that the low-frequency peak does not show any splitting within the resolution of the Fourier transform at any density; this observation indicates that the densities of states and therefore the effective masses of electrons in the two occupied valleys are the same, consistent with the 2DES occupying two nearly degenerate valleys whose principal axes lie in the 2D plane.

Figure 1 reveals that, at high B_{\perp} , all the ρ_{xx} minima become stronger than their $(\nu+4)$ counterparts. For example, the ρ_{xx} minimum at $\nu = 9$ is deeper than the

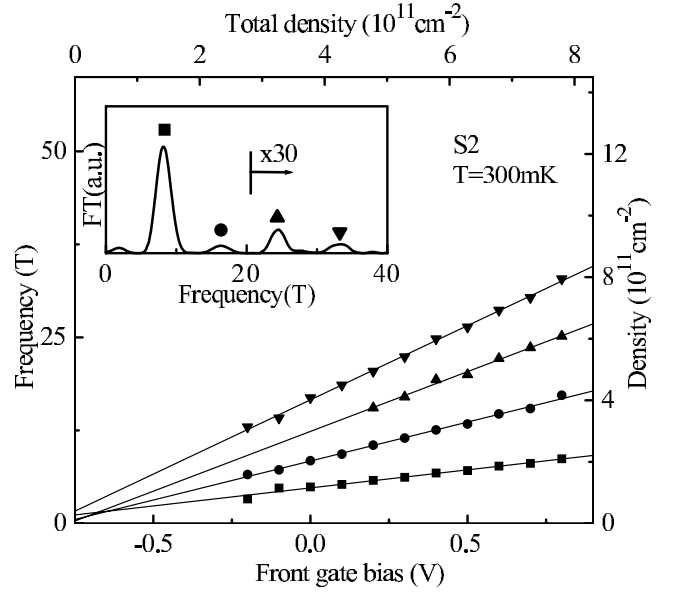


FIG. 2: Inset: An example of the Fourier transform of ρ_{xx} vs. $1/B_{\perp}$ for sample S2 at $n = 7.9 \times 10^{11} \text{ cm}^{-2}$. The presence of a peak at the frequency equal to one quarter of frequency associated with the total density confirms the degeneracy of the spin and valleys at low B_{\perp} . Main: Fourier transform peak frequencies as a function of the front-gate bias.

minimum at $\nu = 13$, while at $\nu = 17$ there is no visible minimum. This progression suggests that all the three relevant energies in the system, i.e., the cyclotron energy, Zeeman energy, and ΔE_V , increase with increasing B_{\perp} . Our coincidence measurements, summarized in Fig. 3(a), provide for a quantitative determination of the energies. This figure, which is the highlight of our study, shows a (color) plot of ρ_{xx} vs. $1/\cos\theta$ (x-axis) and filling factor, ν (y-axis). The plot was made by taking magnetoresistance traces at 32 different θ 's. A striking alternating diamond pattern emerges in the data. This pattern also has periodicity of four in ν . Surprisingly, the pattern changes very little over the (B, θ) parameter space; as shown later, this observation implies that ΔE_V increases approximately linearly with B_{\perp} . Such a dependence leads to the simple energy fan-diagram shown in Fig. 3(b). Another prominent feature of the pattern is its right-left symmetry, which indicates that ΔE_V is independent of B_{\parallel} .

In order to make a quantitative analysis of the data, we assume a general model for the energies of a two-valley system tilted in a magnetic field:

$$E_1 = (N + \frac{1}{2}) \frac{\hbar e B_{\perp}}{m_0 m^*} \pm \frac{1}{2} |g^*| \mu_B \frac{B_{\perp}}{\cos\theta} - \frac{\Delta E_V}{2} \quad (1)$$

$$E_2 = (N' + \frac{1}{2}) \frac{\hbar e B_{\perp}}{m_0 m^*} \pm \frac{1}{2} |g^*| \mu_B \frac{B_{\perp}}{\cos\theta} + \frac{\Delta E_V}{2}, \quad (2)$$

where E_1 and E_2 are the energy levels of valleys 1 and 2, respectively, N and N' are the LL indices, and g^*

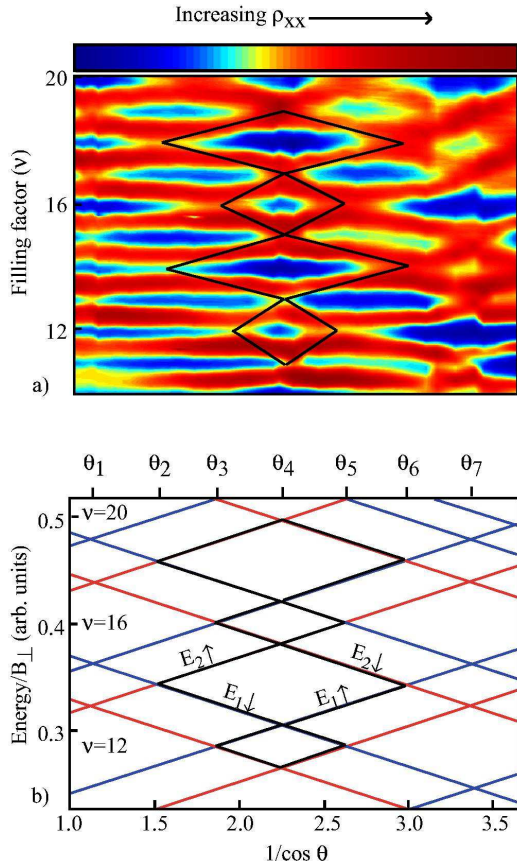


FIG. 3: a) Magnetoresistivity ρ_{xx} vs. $1/\cos\theta$ and ν measured in sample S3 at $T=30\text{mK}$. Blue and red colors represent small and large values of ρ_{xx} , respectively. To increase the visibility of ρ_{xx} oscillations over the whole field range, we scaled ρ_{xx} by a Dingle-like factor, $\exp(1/6.4B_{\perp})$. A striking alternating diamond pattern emerges in the data. This pattern has an approximate right-left symmetry, has a periodicity of four in ν , and changes little over the whole field range. b) Fan diagram that qualitatively accounts for the data. In this diagram, ΔE_V scales linearly with B_{\perp} and is independent of B_{\parallel} .

is the effective g-factor [12]. By fitting the coincidences between energy levels of the same valley using this model, we can determine the Zeeman energy (in units of the cyclotron energy), or equivalently the product $|g^*|m^*$, as a function of B_{\perp} and B_{\parallel} . Likewise, from the coincidences between the energy levels of the different valleys, we can determine ΔE_V (in units of the cyclotron energy), or equivalently, the product $m^*\Delta E_V$.

We first determine the product $|g^*|m^*$ directly from coincidence angles θ_1 , θ_4 , and θ_7 in Fig. 3(a); these angles correspond to the crossings between the LLs associated with the same valley. We find that, at low fields, $|g^*|m^*$ is constant, identical for both valleys, and at $n = 9.55 \times 10^{11} \text{ cm}^{-2}$ equal to 1.76 ± 0.02 . Surprisingly, while $|g^*|m^*$ is

enhanced with respect to its band value of 0.92, it does not oscillate as function of ν contrary to the theoretical expectation [8]. Papadakis *et al.* [4] have also observed a constant enhancement of $|g^*|m^*$ in low density ($n = 2 \times 10^{11} \text{ cm}^{-2}$) AlAs 2D electrons for $\nu \geq 9$. In the higher density samples that we have studied, however, we find a monotonic increase in $|g^*|m^*$ for $\nu < 7$. Here we limit our determination of ΔE_V to the field range where the measured $|g^*|m^*$ is constant.

Next, we determine ΔE_V from the values of angles $\theta_2, \theta_3, \theta_5$ and θ_6 at which the energy levels of different valleys overlap. Since we do not know exactly the absolute LL index, but only the difference between the indices of LLs to which these energy levels belong, ΔE_V can be determined only to within an additive term $2l\hbar e B_{\perp}/m^*m_0$, where l is an integer. In sample S2, the presence of coincidences at θ_2 for low ν (not shown) requires l to be zero. For sample S3, coincidences indicate that the system is not valley-polarized for $\nu \geq 8$. This observation restricts l to either zero or one. We chose zero, since $l = 1$ implies the unlikely situation that valley splitting first shrinks to zero and then increases as a function of B_{\perp} .

Valley splitting measured for samples S2 and S3 is summarized in Fig. 4. Since ΔE_V does not vary with the coincidence angle, it is independent of B_{\parallel} [13]. Furthermore, ΔE_V for different samples and densities fall on the same curve which exhibits a nearly linear dependence on B_{\perp} for $B_{\perp} > 1.5\text{T}$. A least squares fit of the data in this high-field range gives $\Delta E_V = -0.22 + 0.25B_{\perp}$ (assuming $m^* = 0.46$), with ΔE_V in units of meV and B_{\perp} in units of Tesla. At low fields, ΔE_V deviates from the linear behavior.

Two features of the data in Fig. 4 are noteworthy. First, since the widths of the LLs do not affect the positions of the coincidences, there should be no disorder corrections to the plotted values of ΔE_V [14]. Second, the fact that ΔE_V appears to be independent of density and B_{\parallel} , and depends only on B_{\perp} , suggests that electron-electron interaction is responsible for its enhancement with B_{\perp} . The linear dependence on B_{\perp} , on the other hand, is puzzling; one would normally expect a $B^{1/2}$ dependence as the enhancement should inversely scale with the magnetic length. We hope that the results presented in this Letter will serve as incentive for developing a theory to explain the enhancement of valley-splitting in a magnetic field.

We acknowledge the NSF support for this work. Part of the measurements were performed at the NSF-supported National High Magnetic Field Laboratory in Tallahassee, Florida; we thank E. Palm and T. Murphy for technical assistance. We would also like to thank D. Tsui for helpful discussions.

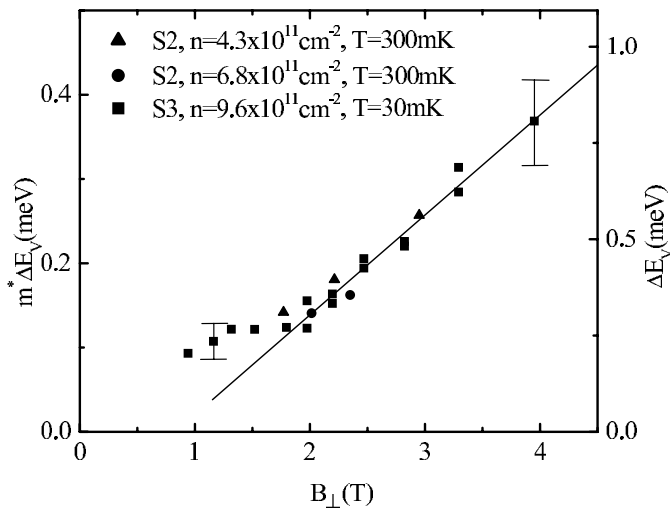


FIG. 4: Products $m^* \Delta E_V$ and ΔE_V (assuming $m^*=0.46$) as a function of B_{\perp} with typical error bars. Solid line is the least squares linear fit for the high field valley splitting.

- [1] T. Ando, A. B. Fowler, and F. Stern, *Rev. Mod. Phys.* **54**, 437 (1982).
 [2] E. P. D. Poortere, Y. P. Shkolnikov, E. Tutuc, S. J. Pa-

- padakis, M. Shayegan, E. Palm, and T. Murphy, *Appl. Phys. Lett.* **80**, 1583 (2002).
 [3] K. Maezawa, T. Mizutani, and S. Yamada, *J. Appl. Phys.* **71**, 296 (1992).
 [4] S. J. Papadakis, E. P. D. Poortere, and M. Shayegan, *Phys. Rev. B* **59**, R12743 (1999).
 [5] T. S. Lay, J. J. Heremans, Y. W. Suen, M. B. Santos, K. Hirakawa, and M. Shayegan, *Appl. Phys. Lett.* **62**, 3120 (1993).
 [6] T. P. Smith, W. I. Wang, F. F. Fang, L. L. Chang, L. S. Kim, T. Pham, and H. D. Drew, *Surf. Sci.* **196**, 287 (1988).
 [7] F. F. Fang and P. J. Stiles, *Phys. Rev.* **174**, 823 (1968).
 [8] T. Ando and Y. Uemura, *J. Phys. Soc. Jpn.* **37**, 1044 (1974).
 [9] We determine the total 2D electron density from either the Hall coefficient or the positions of quantum Hall states which are observed at higher B_{\perp} .
 [10] As will become clear later in the paper, whether the strongest minima occur at $\nu = 8, 12, 16$, etc., or at $\nu = 10, 14, 20$, etc. depends on the relative strengths of the cyclotron and Zeeman energies.
 [11] The peak near zero frequency is an artifact of the window and the range used in taking the Fourier transform.
 [12] As we show later, g^* is the same for both valleys.
 [13] For example the two data points at $B_{\perp}=2.82 \text{ T}$ are from coincidences at $\theta = 47^\circ$ and $\theta = 71^\circ$.
 [14] The FWHM of the electron wavefunction in our samples is likely less than 50 \AA , so that corrections for the effects of the finite layer thickness are less than 1% of ΔE_V .